Transactions of the 17th International Conference on Structural Mechanics in Reactor Technology (SMiRT 17)
Prague, Czech Republic, August 17 –22, 2003
Paper # H04-2

Ultimate Resistance of a Reinforced Concrete Foundation Under Impulsive Loading

Donato Aquaro[1)], Giuseppe Forasassi[1)], Massimo Marconi[1)]

[1)] Department of Mechanical, Nuclear and Production Engineering, University of Pisa, Italy.

ABSTRACT

This paper deals with numerical simulations of the ultimate resistance of a reinforced concrete foundation under impulsive loading.

The research program, which is being carried out at the University of Pisa, aims to assess the capability of multi purpose F.E.M. codes to simulate the behaviour of reinforced concrete under impulsive loads and in non linear conditions.

In this paper , the impact of a spent nuclear fuel cask against a reinforced concrete slab of a temporary repository for spent nuclear fuel is numerically analysed . The analysis considers accidental events in which a spent nuclear fuel cask would drop against the floor of a repository during lifting operations.

Two types of solutions have been taken into account: a simple reinforced concrete structure and a structure provided with a 40mm thick steel liner on the impacted surface, connected to a 1600mm thick concrete bed.

The model is assumed to be axis symmetric and positioned on an elastic ground (Winkler model). The concrete has been simulated as: - elastic perfectly plastic under compressive stresses limited by a crushing strain; elastic linear under tensile stresses until a cracking stress value and a following decrease of stress characterized by a constant or variable softening modulus; limited ability to resist at shear stresses after cracking characterized by a shear retention factor. The steel of the reinforcement bars and of the cask has been simulated as an elastic perfectly plastic material.

Several numerical simulations have been performed in order to determine the influence, on the ultimate resistance of the structure under examination, of the steel liner, of some characteristic parameters of concrete (as the softening module and the shear retention factor) and of the Winkler coefficient values, simulating the elastic behaviour of the ground.

The obtained results demonstrate that a steel liner produces a lower stress in the concrete as well as in the reinforcement but the bed is still subjected to the cracking phenomenon throughout its entire width although the crushing is localized to only a few elements near the impact zone.

The use of a more complex constitutive equation for the concrete considering the shear retention factor and the softening module has given results which do not differ greatly from those related to a more simplified model. A different degree of stiffness of the ground has a greater influence on the behaviour of the concrete bed.

The FEM code , mainly used in the analyses illustrated in this paper, is the MARC [1]. The on-going activities include the use of the F.E.M. computer code EUROPLEXUS [2](developed jointly by the Commissariat a l'Energie Atomique and by the European Commission) which is able to elaborate complex 3D structures and to consider different types of constitutive equations.

KEY WORDS: impact,, concrete, crushing strain, cracking stress, shear retention factor, softening module, Winkler coefficient, F.E.M, spent nuclear fuel cask.

1. INTRODUCTION

The behavior of the concrete is very complex before the failure occurs as well as after. Some phenomena that make the mathematical description of the concrete complicated are the following: the different resistance and the different failure modes under tensile or compressive stresses , the material softening after the cracking or the crushing, the partial resistance under shear stresses after the cracking. Many authors have suggested several constitutive equations in order to describe the failure modes of the concrete. These equations need the knowledge of material constants (characteristics of the different failure modes) which are not easy to determine experimentally given that they involve three dimensional stress state.

1.1 Behavior of the concrete under uniaxial loading

A typical concrete stress-strain curve under uniaxial loading is shown in Fig. 1. The stress-strain curve is generally nonlinear in compression. However, when stress is less than 30% of the maximum compressive strength the stress-strain behaviour is almost linear. As the load is increased, however, the tangent of the stress-strain curve continuously decreases and it becomes zero at the maximum compressive strength. At about 75%-90% of this peak value, small

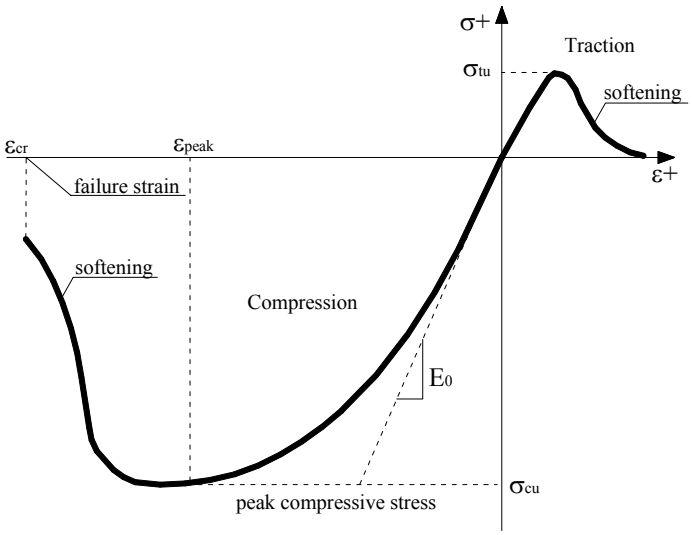

Fig. 1: Typical Stress-Strain curve for concrete.

cracks or fissures appears on the surface of the concrete test specimen. After the peak value, the stress decreases along a curve named softening curve and the crushing failure occurs when the strain reaches the value ε_{cr}, that is the crushing strain.

The peak value of the compressive stresses can be approximated by means of the characteristic cube strength of the concrete. The concrete Italian rules gives the following relations: $E_o = 5692\sqrt{\sigma_{cu}}$ MPa, for the elastic modulus (linear part of the stress-strain curve) while the strain crushing ranges between 0.003 and 0.0035.

In the tensile regimen , the maximum tensile strength, σ_{tu}, is called the cracking stress and it ranges between 0.05-0.1 the maximum compressive strength ($0.05\sigma_{cu}$ for high strength concrete and $0.1\sigma_{cu}$ for medium strength concrete).

Usually concrete in tension is modelled as a linear elastic strain softening material. The cracking stress produces a crack perpendicular to the stress direction and after the crack occurs the tensile stress can go immediately to zero or it can vanish along a softening curve .

$$\sigma = \sigma_{tu} \cdot e^{-\frac{\varepsilon - \varepsilon_{cu}}{\alpha}}$$

Petersson [3], [5] formulated the following strain softening model (Figure 2):

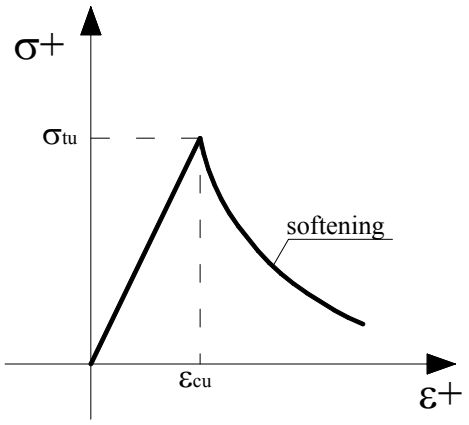

Fig. 2: Tensile strain softening model for concrete.

eq. 1)

where:

ε is the tensile strain in the cracked zone,

ε_{cu} is the corresponding cracking strain, α is the softening parameter given by:

$$\alpha = \frac{G_f - \frac{\sigma_{tu} \cdot \varepsilon_{cu} \cdot l_c}{2}}{\sigma_{tu} \cdot l_c} > 0$$

$$l_c = \frac{volume\ \ containing\ \ a\ crack}{area\ \ of\ \ crack} = \frac{V}{A_{cs}}$$

$$G_f = \int_0^{\infty} \sigma(\omega) \cdot d\omega$$

is the fracture energy needed to form the fracture surfaces (50÷200 N/m)

$\omega = l_c\, \varepsilon_{cu}$ is the crack width.

The softening curve could be approximated by means of a linear function obtained considering the tangent of the exponential curve in Figure 2 in the point (σ_{tu}, ε_{cu}).

In a three dimensional stress state , the crack could close and support shear stress by means of friction.

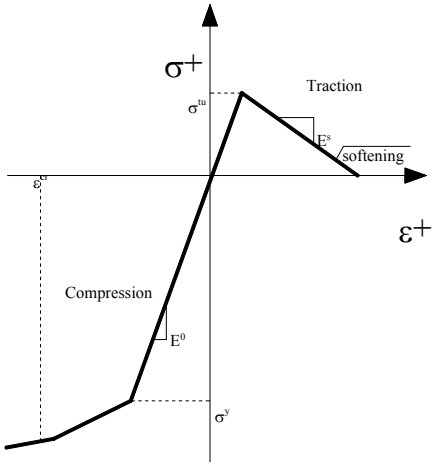

Fig. 3: Uniaxial stress-strain diagram.

1.2 Numerical simulation of the concrete

The numerical simulations of the ultimate resistance of a concrete foundation, illustrated in this paper, have been performed using the FEM code Marc. In this code, the concrete constitutive equation illustrated graphically in Figures 1 and 2 can be easily implemented by means of user routine. Moreover the simplified

model, shown in Figure 3, can be chosen as default for simulating low tension material. This model permits the analysis of the crack initiation (when in a principal direction the principal tensile stress becomes equal to the cracking stress) and simulates the tension softening, considering a linear behaviour characterized by means a softening modulus E_s. On the basis of the equation 1), the softening may be dependent upon the element size (the l_c term in the eq.1). After a crack forms, the loading can be reversed and the crack can close again (depending on the opening distance of the crack). In this case, the crack has full compressive stress-carrying capability and the shear stress is transmitted over the crack surface by friction, therefore with a reduced shear modulus. The shear retention factor indicates the capability of transmitting shear stress over the crack surface. The values of this factor range between 0.0÷0.5.

In the compressive state the concrete is simulated as an elastic plastic material with work hardening. The material loses its integrity and the capability of carrying a load when a crushing strain value is reached.

2. ANALYSIS OF A CONCRETE FOUNDATION UNDER IMPULSIVE LOADS

The numerical analyses have the aim of verifying the integrity of the concrete foundation (modelled as a thick plate) of a nuclear spent fuel temporary storage building hit by a cask.

The temporary storage building taken into consideration measures 45m x 50m and the floor is made up of a reinforced concrete foundation about 1600mm thick. The impact velocity of the cask has been assumed to be equal to 3.14m/s correspondent to a drop height of 0.5m. The characteristics of the cask used in the analyses are those of the AGN-1 cask (Figure 4). The numerical simulations were carried out considering different geometric configurations of contact between the cask and the concrete floor.

The simulated event corresponds to a free drop accident during the movement of the nuclear spent fuel casks. The casks are moved using a gantry crane.

The maximum distance between the cask bottom and the floor during the movement is 0.5m. In the case of failure of the lifting structure the cask may drop against the floor.

Should this kind of event occur, the damage to the floor must not endanger its structural function and its leak tightness characteristics.

As the data for the casks which will actually be used for the storage of the Italian nuclear spent fuel are not available, the AGN-1 cask was chosen despite having some notable differences from the casks which will actually be used as regards dimension and weight.

The AGN-1 has a total weight of about 54t without the shock absorbers located at the extremities. It is about 4m high and its maximum diameter is about 1.5m.

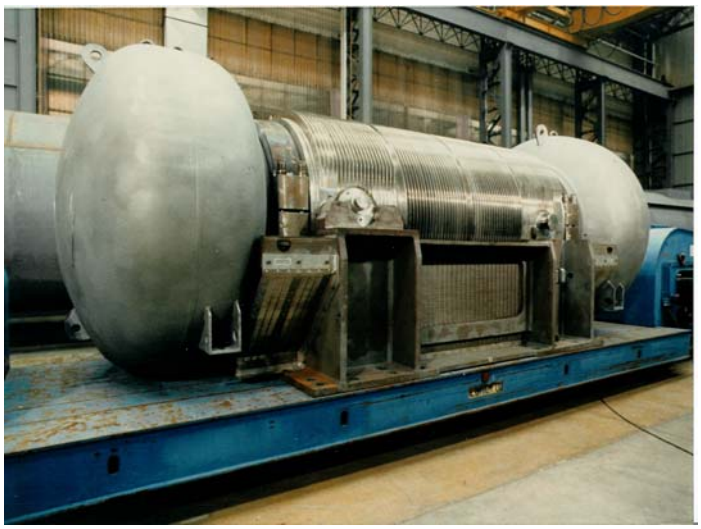

Fig. 4: AGN-1 cask with shock absorber.

2.1 NUMERICAL MODEL OF THE CASK AND THE CONCRETE FOUNDATION

The numerical model was implemented making the following assumptions:

- both the cask and the concrete foundation can be simulated by an axis symmetric mesh ;
- the concrete floor is constrained only by the ground and the tying coming from the building structure are not considered;
- in the range of the compressive stresses, the concrete is considered an elastic-perfectly plastic material;
- the steel of the reinforced bars and of the cask is considered an elastic-perfectly plastic material not rate sensitive;
- the cask hits the concrete floor with its axis perpendicular to the floor.

2.1.1 Model of the cask

The cask is essentially a cylindrical body with a cylindrical cavity inside. It was simulated with an axis symmetrical mesh made of 1114 ring elements (type 10 of the MARC code) with sides measuring 3.50cm x 3.85cm (Figure 5). The cask model does not take into consideration certain details such as the refrigeration fins, the internal components (rack, valves etc.). Moreover the stiffness of the fuel elements inside the cask was neglected but the mass was concentrated on the nodes of the internal cavity (mass of 126Kg weights were placed on each of the 115 nodes).

The contact between the cask and the floor was simulated by means of constraints reacting only at compressive loads without any friction. The nodes on the symmetrical axis (axis z) having a zero radial coordinate were blocked radially to respect the axisymmetric assumption of the problem.

The cask is made of ASME SA 350 gr LF1 steel, which was simulated as an elastic-perfectly plastic material with the following mechanical characteristics:

Young's modulus E = 210Gpa, Poisson's coefficient ν = 0.3, density ρ = 7800Kg/m^3, yield stress σ_y = 205MPa.

2.1.2 Model of the reinforced concrete floor

Two different types of concrete floor were considered. The first one is a simple reinforced concrete floor while the second has a liner made of a 4cm thick steel plate. The steel plate was located between the upper reinforced concrete surface and the cask. The floor model has a radius of 10m and a thickness of 1.6m and lies directly on the ground.

In order to increase the accuracy of the results of the analysis the portion of the floor directly involved in the impact (having a radius of 2m) was simulated with a finer mesh made of 2000 axisymmetric elements 4cm x 4cm of side.

The remaining part of the floor (from r = 2m to r = 10m) was meshed with 2000 axisymmetric elements 8cm x 8cm of side (Figure 5).

The reinforcement bars, located in the radial and circumferential direction, are made up of bars Ø = 26mm of diameter, p = 150mm of horizontal pitch and an axial distance between the layers of reinforcement bars equal to 80mm.

A mesh of 4000 axis symmetric elements was created for the reinforcement (REBAR elements type 144 MARC code). Even although the REBAR element is defined as independent, it has the same dimensions as the concrete element on which it is placed and it also shares the same 4 nodes.

As regards the floor lined with a steel plate, this plate is divided into 250 axis symmetric elements (type 10) 4cm x 4cm of side.

The constraints of the floor are the following:

- a radial constraint (radial displacement zero) of the nodes at r = 0.0m, which simulates the axial symmetry of the model;
- a radial constraint (radial displacement zero) of the nodes at r = 10m, which simulates the tying due to the concrete material located at the edges of the floor, neglected in the model (the model considers only a part of the floor);
- the axial constraint , due to the presence of the ground, applied to the node located at the bottom of the model (nodes having coordinate z = 0.0m).

The floor lies on a ground simulated as an elastic soil , characterised by a constant stiffness, K (this soil is called Winkler soil).

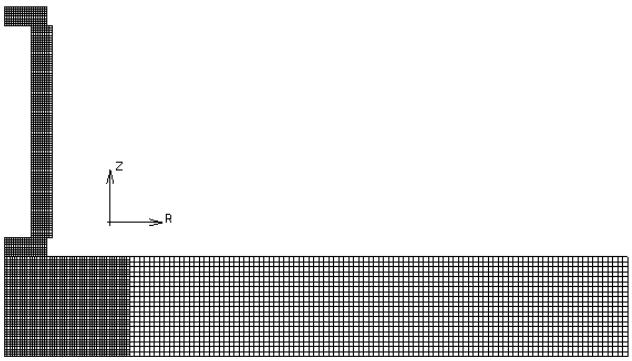

Fig. 5: Cask and concrete floor model.

As previously mentioned, the concrete was simulated as an elastic-perfectly plastic material under compression and as a linear elastic with linear softening in traction. The failure under compressive stresses occurs when the strain exceeds the crushing strain ε_{cr}. The traction resistance is limited by the cracking stress σ_{tu}.

The mechanical characteristics of the concrete are as follows:

Young's modulus E = 33GPa, Poisson's coefficient ν = 0.17, density ρ = 2340Kg/m^3, yield stress σ_y = 28 MPa;

Crushing strain ε_{cr} = 0.0035, critical cracking stress σ_{tu} = 4.17 MPa, softening modulus E_s = 1.79 GPa.

The reinforcement bars made of Feb44k steel were simulated as an elastic-perfectly plastic material with the following mechanical characteristics:

Young's modulus E = 210GPa, Poisson's coefficient ν = 0.3, density ρ = 7800Kg/m^3, yield stress σ_y = 421.4MPa.

3. MAIN OBJECTIVES OF THE NUMERICAL ANALYSES

The main objectives of the numerical analyses were to determine the influence of certain parameters (mechanical characteristics of concrete, soil stiffness, contact surface between cask and floor) on the results in order to analyse the dynamic behaviour of the floor, to evaluate the damages caused to it from the impact of the cask and to check the capability of the MARC code to simulate the actual behaviour of the concrete.

Eight transient analyses were carried out taking into consideration two different types of floor (with and without the steel plate liner). The first floor is a simple reinforced concrete structure while the second contains a steel plate, 4cm thick, placed between the cask and the concrete upper surface of the floor. Moreover the values of some parameters of the concrete constitutive equation have been changed.

The first one is the ***shear retention factor τ***, which is the material's capacity to transmit the shear stress after the formation of the crack and its successive closure .

The second parameter varied is the ***softening module E_s***, which is the material's capacity to support tensile stress, in reduced manner, after the cracking phenomenon is occurred.

The final parameter considered in the analyses is the ***Winkler coefficient K*** in relation to the behaviour (stiffness) of the ground on which the floor lies. Two distinct values for this variable were adopted which represent the two following types of ground :

- Compact clay of normal consolidation, medium loose sand simulated by a stiffness of $2.0\ 10^7$ (N/m x m^2)
- Compact clay of high consolidation, very compact sand or gravel simulated by a stiffness of $2.0\ 10^8$ (N/m x m^2).

Table 1 shows a summary of the eight transient analyses performed.

Table 1: The eight dynamic analyses conducted.

	Concrete bed without plate				*Concrete bed with plate*			
ID Analysis	***1st***	***2nd***	***3rd***	***4th***	***5th***	***6th***	***7th***	***8th***
Winkler coefficient K *(N/m)(1/m²)*	$2.0\cdot10^7$	$2.0\cdot10^7$	$2.0\cdot10^8$	$2.0\cdot10^8$	$2.0\cdot10^7$	$2.0\cdot10^7$	$2.0\cdot10^7$	$2.0\cdot10^8$
Shear retention factor τ	0.5	0.1	0.1	0.0	0.0	0.1	0.1	0.1
Softening module E_{soft} *(GPa)*	0.0	0.0	0.0	0.0	0.0	0.0	1.79	1.79
Period analysis ΔT *(msec)*	9.6				13.2			

4. MAIN RESULTS OF THE ANALYSES

The following paragraphs illustrate some of the most interesting results obtained from the analyses performed.

Figure 6 shows the first six modes of the model without the steel plate liner, while table 2 reports the first ten natural frequencies of the two models taken into consideration. The value of the tenth natural frequency for both models is about 500Hz, therefore the damping chosen for the analyses damps the oscillations having frequency equal to 1000Hz with a damping coefficient of 1%. This is produced choosing a stiffness damping with $\beta=3.2\ 10^{-6}$, on the basis of Rayleigh's hypothesis. Consequently the time step was fixed at 10^{-5} sec.

Table 2: Natural frequencies of system.

	Frequency [Hz]									
Concrete bed without steel plate	10.09	36.25	98.34	168.8	227.5	247.0	336.6	415.8	432.6	529.0
Concrete bed with steel plate	10.04	23.77	79.55	115.7	147.3	222.6	311.3	320.3	405.3	498.1

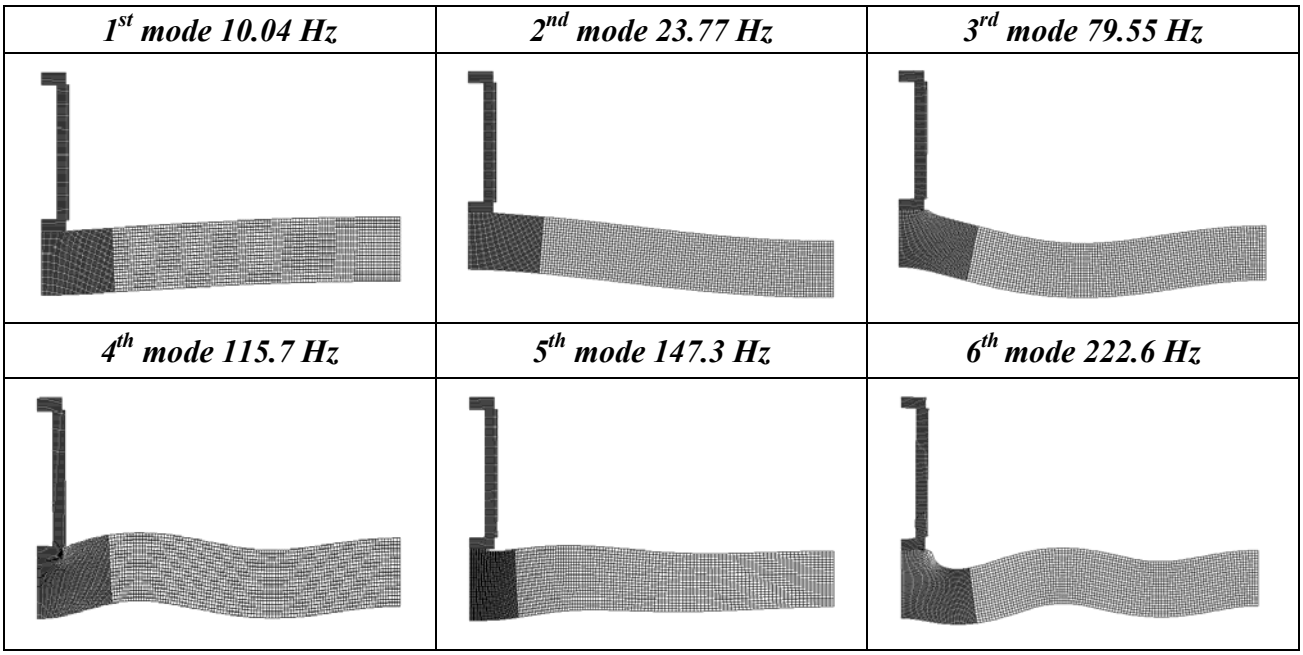

Fig. 6: First six modes of the model without the steel plate liner.

The shear retention factor, related to the concrete behaviour, plays an important role in the absorption of the cask's kinetic energy and in the deformations of the various components of the system, above all for high values of soil stiffness.

Figures 7 and 8 compare the energies absorbed by the concrete (Figure 7) and by the soil (Figure 8) for two values of shear retention factor. The results shown correspond to the analyses n^{os}. 3 and 4. Increasing the shear retention factor increases the absorption of energy of the concrete as deformation energy and a correspondingly more rapid deceleration of the cask. Conversely, a zero value for this parameter produces an increase in the elastic deformation energy of the soil (Figure 8).

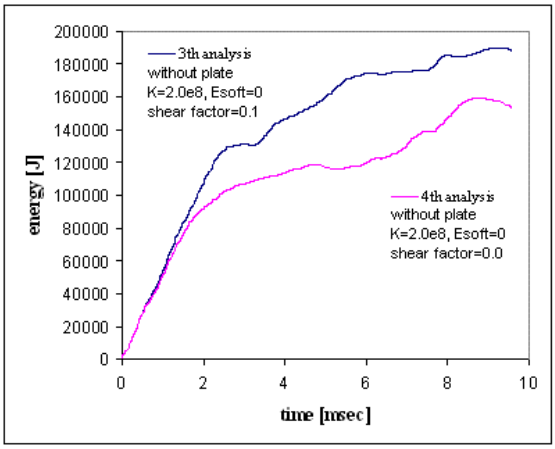

Fig. 7: Comparison between concrete energy deformation versus time for different shear retention factor.

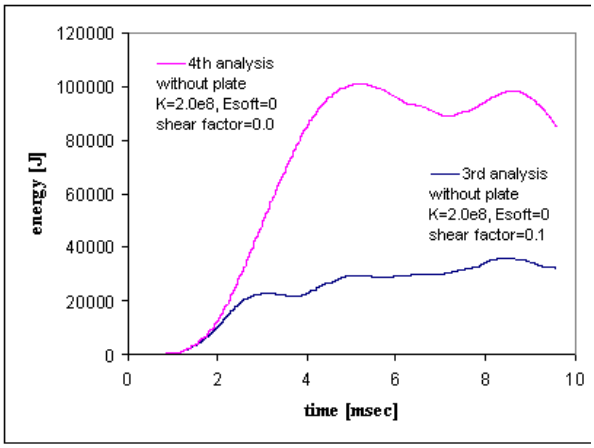

Fig. 8: Comparison between soil energy deformation versus time for different shear retention factor.

When a non-zero value of the softening module is introduced, a different stress level is obtained in the liner steel plate , obviously only after the cracking is developed (after 2.0msec) (Figure 9).

In both cases, in the area involved in the contact, the material yields but in the non-zero softening module the stresses are reduced more quickly and the plastic strain are notably less.

The presence of the steel plate liner greatly reduces the stress level in the reinforcement bars.

Figure 10 shows the stresses in the reinforcement bars located in circumferential direction in the lower part of the floor.

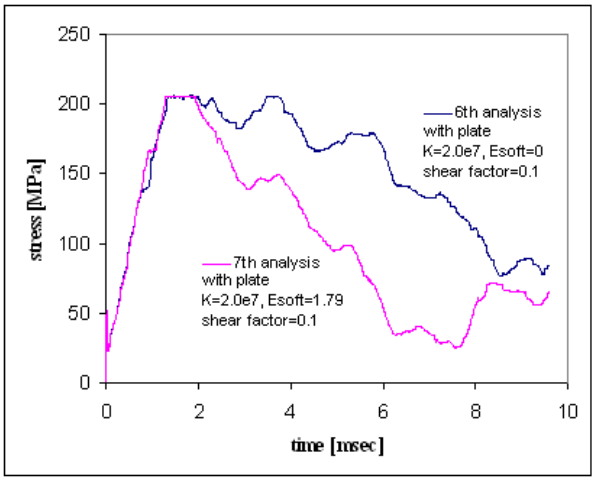

Fig. 9: Comparison between plate Von Mises stress versus time for different softening modulus r=0.8m top of model.

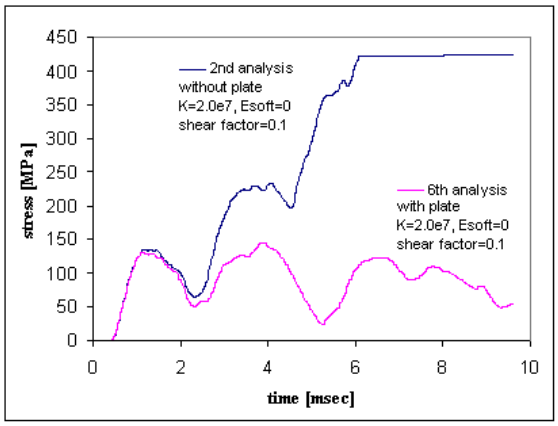

Fig. 10: Comparison between steel bar stress versus time for different bed (bars located in circumferential direction at the bottom of the concrete bed).

Figure 11 illustrates the Von Mises stress contour bands of the concrete elements in the first 2m of the reinforced concrete floor at the final instant of the analyses. Figure 11 shows the elements in which the crushing phenomenon was developed.

Concrete bed without metal plate

	Analysis 1	***Analysis 2***	***Analysis 3***	***Analysis 4***
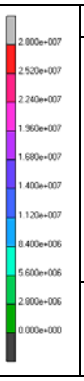	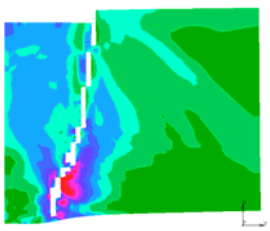	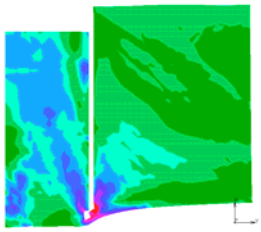	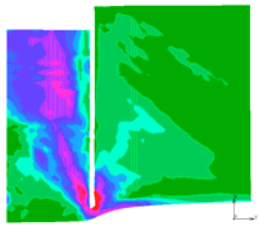	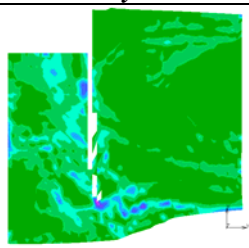
	K = 2.0e7 *(N/m)(1/m²)* ***τ = 0.5*** E_{soft} ***=0.0*** *(GPa)*	***K = 2.0e7*** *(N/m)(1/m²)* ***τ = 0.1*** E_{soft} ***=0.0*** *(GPa)*	***K = 2.0e8*** *(N/m)(1/m²)* ***τ = 0.1*** E_{soft} ***=0.0*** *(GPa)*	***K = 2.0e8*** *(N/m)(1/m²)* ***τ = 0.0*** E_{soft} ***=0.0*** *(GPa)*

Concrete bed with metal plate

	Analysis 1	***Analysis 2***	***Analysis 3***	***Analysis 4***
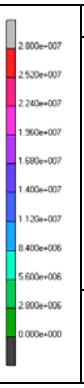	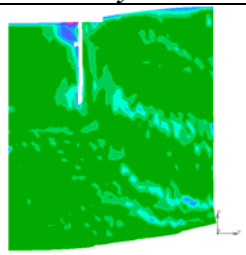		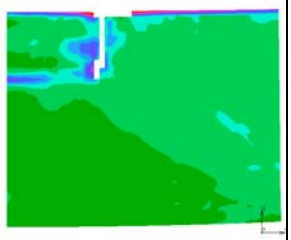	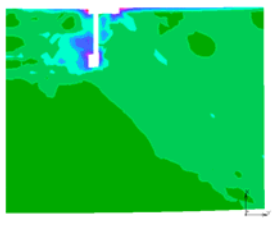
	K = 2.0e7 *(N/m)(1/m²)* ***τ = 0.0*** E_{soft} ***=0.0*** *(GPa)*	***K = 2.0e7*** *(N/m)(1/m²)* ***τ = 0.1*** E_{soft} ***=0.0*** *(Gpa)*	***K = 2.0e7*** *(N/m)(1/m²)* ***τ = 0.1*** E_{soft} ***=1.79*** *(GPa)*	***K = 2.0e8*** *(N/m)(1/m²)* ***τ = 0.1*** E_{soft} ***=1.79*** *(GPa)*

Fig. 11: Crushing phenomenon in concrete.

In the case of the floor without the steel plate the crushing occurs mostly on a cylindrical surface, having radius equal to that of the cask and involving almost the entire thickness of the floor. In the floor with the plate the crushing is much more limited. It develops radially during the transient, penetrating the floor for about 60cm. Obviously the mean acceleration of the cask is greater with the steel plate liner than without it (Figure 12 and Table 3)

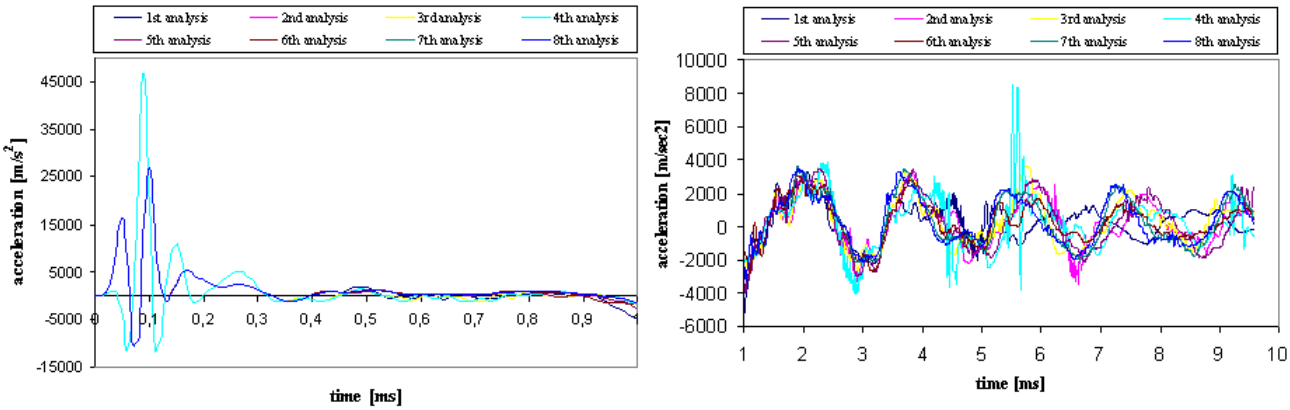

Fig. 12: Acceleration of the cask.

Table 3: The average acceleration averages of the cask.

	Concrete bed without plate				*Concrete bed with plate*			
ID Analysis	***1st***	***2nd***	***3rd***	***4th***	***5th***	***6th***	***7th***	***8th***
Average deceleration of the tank *(g)*	39	32	39.5	31	73.6	74.3	88.8	94.1

5 CONCLUSION

The following important indications for the design of the structure can be drawn from the results obtained.

- The introduction of the upper steel plate, as could be logically expected, allows the stress generated in the concrete and reinforcement to be distributed more uniformly. An evident consequence of this is the notable reduction in the concrete crushing, which in the floor without the plate involves its entire thickness (1.6m).
- The presence of the upper steel plate also reduces the stress in the reinforcement bars . The yielding of the steel material, present in the reinforcement bars in the lower part of the floor, which were the most solicited in all the simulations carried out, disappears in the floor lined with the steel plate.
- Although the reinforcing plate reduces the damage to the floor, cracking still occurs along its entire thickness. Differently from the floor without the plate, if there was a radioactive release inside the store, any cracks created in the concrete would not be dangerous as the plate would act as a barrier.
- The use of a more complex constitutive equation for the concrete, introducing shear retention and a softening module did not give results that were very different from a simpler model. Nevertheless the damage in terms of crushing and cracking is reduced considering zero values of these parameters.
- More accurate results could be obtained using a model for the materials which is closer to reality, considering also the effects of strain rate.
- Different constraint conditions, characterised by the stiffness of the ground, have a notable influence on the behaviour of the floor and of cask acceleration.

REFERENCES

[1] Marc Analysis Corp., “User Manual” Vol. A, Palo Alto Ca, 1998.
[2] Europlexus “User’s Manual” ,Commissariat a l’Enerigie Atomique, European Commision J.R.C., 2002.
[3] Petersson J., “Crack growth and development of fracture zones in plain concrete and similar materials”, PhD Thesis, University of Lund, 1981.
[4] Aquaro D., Forasassi G., Castrataro P. “Impact Resistance of a Concrete Bed for a pent Nuclear Fuel Cask Repository”, SMiRT 16, Washington, DC USA, August 12-17, 2001.
[5] Bangash M.Y.H., “Concrete and Concrete Structure: Numerical Modelling and Applications”, Elsevier Applied Science, London and New York, 1989.